Biochemical and Biophysical Research Communications 423 (2012) 386–391

Contents lists available at SciVerse ScienceDirect

Biochemical and Biophysical Research Communications

journal homepage: www.elsevier.com/locate/ybbrc

Engineering of a novel Ca^{2+}-regulated kinesin molecular motor using a calmodulin dimer linker

Hideki Shishido, Shinsaku Maruta *

Department of Bioinformatics, Faculty of Engineering, Soka University, Hachioji, Tokyo 192-8577, Japan

ARTICLE INFO

Article history:
Received 15 May 2012
Available online 1 June 2012

Keywords:
Calmodulin
Dimer
Kinesin
Molecular shuttle
Motor protein

ABSTRACT

The kinesin–microtubule system holds great promise as a molecular shuttle device within biochips. However, one current barrier is that such shuttles do not have "on–off" control of their movement. Here we report the development of a novel molecular motor powered by an accelerator and brake system, using a kinesin monomer and a calmodulin (CaM) dimer. The kinesin monomer, K355, was fused with a CaM target peptide (M13 peptide) at the C-terminal part of the neck region (K355–M13). We also prepared CaM dimers using CaM mutants (Q3C), (R86C), or (A147C) and crosslinkers that react with cysteine residues. Following induction of K355–M13 dimerization with CaM dimers, we measured K355–M13 motility and found that it can be reversibly regulated in a Ca^{2+}-dependent manner. We also found that velocities of K355–M13 varied depending on the type and crosslink position of the CaM dimer used; crosslink length also had a moderate effect on motility. These results suggest Ca^{2+}-dependent dimerization of K355–M13 could be used as a novel molecular shuttle, equipped with an accelerator and brake system, for biochip applications.

1. Introduction

Molecular shuttles based on kinesin and microtubules hold great promise in bionanotechnology applications such as nano-electromechanical systems (NEMS) and biochip devices in which kinesin is coated on a glass surface and microtubule gliding over the surface is observed [1,2]. NEMS and biochips are devices that integrate electrical and mechanical functionality on the nano- or micro-scale. Dekker [3] and Hess [4,5] have reported the many roles of kinesin as active components in such systems. For example, a kinesin molecular shuttle has been proposed as part of a "smart dust" biosensor [6]. To achieve high functionality or high capability, kinesin molecular shuttles require additional modifications. For instance, a cargo-loading system is necessary for application of the kinesin–microtubule transport system to NEMS or biochip devices [7]. However, the ability to reverse such a cargo-loading system has not been reported. Recently, we overcame this issue by development of a molecular shuttle with a reversible cargo-loading system using calmodulin (CaM) and CaM target peptide (M13 peptide) [8]. Another desirable feature is an accelerator and brake reversible system. In this regard, caged ATP has been used as an accelerator [9] of kinesin; however, the drawback is that the kinesin cannot brake. Konishi et al. introduced a CaM-binding consensus sequence into a region near the microtubule binding site of kinesin in order to regulate kinesin motile in a CaM–calcium dependent manner [10]. However, this did not bring completely arrest kinesin.

Kinesin is a motor protein that moves processively along microtubules, converting the chemical energy of ATP into mechanical energy. The energy conversion efficiency of kinesin-1 is far higher than that of man-made machines. Therefore, it is expected that introduction of artificial switching devices into the functional sites of motor proteins may enable their use as highly efficient bionanomachines. Conventional kinesin-1, a dimeric protein, transports intracellular vesicles along axonal microtubules; structurally, it consists of two heavy and two light chains. Each heavy chain consists of an N-terminal motor domain connected via a neck linker to a α-helical coiled-coil stalk that ends in a C-terminal tail domain formed with a light chain. The motor domain is globular and contains the microtubule- and ATP-binding sites. Kinesin-1 moves along microtubules in >100 consecutive 8-nm steps before dissociating [11,12] and converts the chemical energy of ATP hydrolysis into mechanical energy (~5 pN) [13]. The structure and energy

Abbreviations: CaM, calmodulin; K355, 1–355 amino acid-residue kinesin; K355–M13, K355 with the M13 peptide fused to the C-terminal part of the neck region; NEMS, nano-electromechanical systems; UV, ultraviolet; VIS, visible; BMOE, bis(maleimide)ethane; BMH, bis(maleimide) hexane; $BM(PEO)_3$, 1,11-bis(maleimide) triethyleneglycol; EGTA, ethylene glycol bis (β-aminoethylether)-*N*,*N*,*N*′,*N*′-tetraacetic acid; DMF, *N*,*N*-dimethylformamide; SEC–HPLC, size-exclusion chromatography combined with high-performance liquid chromatography; V_{max}, the maximum enzyme activity of kinesin; K_m[MT], the microtubule concentration when half-maximum activity of kinesin was detected; K560, 1–560 amino acid-residue kinesin; ABDM, 4,4′-azobenzene-dimaleimide.

* Corresponding author. Fax: +81 426 91 9312.
E-mail address: maruta@soka.ac.jp (S. Maruta).

0006-291X/$ - see front matter © 2012 Elsevier Inc. All rights reserved.
http://dx.doi.org/10.1016/j.bbrc.2012.05.135

conversion mechanisms of kinesin have been described at the molecular level [14]. Furthermore, the preparation of recombinant kinesin is comparatively facile using *Escherichia coli* as an expression system. Therefore, one can introduce artificial control systems into the functional regions of kinesin that are related to energy conversion by using genetic engineering techniques and chemical modification methods.

In virtually every eukaryotic cell, CaM plays a significant role in the signaling and regulatory events occurring in many Ca^{2+}-dependent processes. Many of the CaM target proteins are enzymes whose activities are stimulated by binding with CaM in a Ca^{2+}-dependent manner [15,16]. CaM is a relatively small protein consisting of 148 amino acid residues and has two globular domains that are connected to each other by a long central helix. CaM target proteins have relatively short CaM-binding peptides such as M13 peptides and IQ motifs. It has been shown that M13 peptide, which consists of 20 residues and is a part of skeletal muscle myosin light chain kinase, forms a 1:1 complex with CaM in the presence of Ca^{2+} [17]. In a previous study, we successfully controlled the binding function of CaM to M13 peptide by ultraviolet (UV) or visible (VIS) light irradiation using a photochromic compound in order to use as a nanodevice. These results suggest that CaM may be utilized in the development of nanodevices for bionanotechnology applications.

In order to gain more fine control of kinesin motor activity, we developed a novel molecular motor powered by a Ca^{2+}-dependent accelerator and brake system. This molecular motor is composed of two monomeric kinesins fused to an M13 peptide and a CaM dimer. This study demonstrated that kinesin motility was regulated reversibly in an "on–off" fashion by CaM dimers in a Ca^{2+}-dependent manner, and that different types of CaM dimer imparted different velocities to this molecular motor. We suggest this approach will be applicable to other bionanomachines or bionanodevices of NEMS or biochips.

2. Materials and methods

2.1. Expression and purification of recombinant proteins

We constructed the plasmid pET21a (Novagen, Madison, WI, USA), which carried a mouse conventional kinesin construct comprising residues 2–355, a 2 amino acid-residue linker, and the M13 peptide sequence, RWKKNFIAVSAANRFKKIS, with a C-terminal 6× His tag. *E. coli* BL21 (DE3) cells were transformed by the plasmid (pET21a: K355–M13) for expression. K355–M13 was then purified from *E. coli* lysate using Ni-chelating chromatography, followed by dialysis against 100 mM NaCl, 30 mM Tris–HCl (pH 7.5), 0.3 mM $MgCl_2$, 0.2 mM ATP, and 1 mM DTT. Purified K355–M13 was stored at −80 °C until use, as previously described [18]. The ATPase activity of K355–M13 was measured at 25 °C in a reaction mixture comprising K355–M13, 50 mM imidazole–HCl (pH 6.7), 10 mM NaCl, 3 mM $MgCl_2$, 1 mM ethylene glycol bis (β-aminoethylether)-*N*,*N*,*N*′,*N*′-tetraacetic acid (EGTA), 1 mM β-mercaptoethanol, 0.2–10 μM microtubule and 1 mM ATP as described previously [19]. Tubulin was purified from porcine brain, as described by Hackney [20]. The CaM wild type and mutants, Q3C, R86C, and A147C, were prepared as described previously [18].

2.2. Preparation of CaM dimers

CaM mutants were desalted on a Sephadex™ G-50 Fine (GE Healthcare Bio-Science, Piscataway, NJ, USA) column. For the dimerization of the mutated site in CaM, 50 μM CaM mutants and 25 μM crosslinker (BMOE, BMH, or $BM(PEO)_3$) were made to react in 30 mM NaCl, 30 mM Tris–HCl (pH 7.5), and 5% *N*, *N*-dimethylformamide (DMF) for 4–8 h at 25 °C. The crosslinker-mediated dimerization reactions were terminated by the addition of 2 mM DTT. CaM mutant dimers were isolated from the unreacted reagents and CaM mutant monomer, using size-exclusion chromatography coupled with HPLC (SEC–HPLC) as described previously [18]. To confirm dimerization, the eluate peaks from SEC–HPLC were analyzed with SDS–PAGE. The dimerization efficiencies were calculated by measuring the band intensities of CaM dimers and monomers.

2.3. Microtubule gliding assay

Microtubule gliding assays for kinesin were performed as described [21] using assay buffer (50 mM K-acetate, 2.5 mM EGTA, 4 mM $MgSO_4$, 10 mM Tris–acetate (pH 7.5), 0.5% β-mercaptoethanol, and 4 mM taxol) for all solutions at room temperature. Flow cells were constructed using microscope slides, coverslips, and two-sided tape. In brief, glass surfaces of the flow cells were first coated with 0.1% nitrocellulose, and then, 14 μM K355–M13-containing assay buffer was added to the flow cells. The K355–M13 was allowed to adhere to the glass for 5 min. Subsequently, rhodamine-labeled microtubules (∼300 nM rhodamine-labeled tubulin dimer) containing assay buffer were added to the flow cells. The microtubules were allowed to adhere to the glass for 5 min and visualized. Finally, a motility solution (1 mM ATP, 3 mg/ml glucose, 0.02 mg/ml catalase, and 0.1 mg/ml glucose oxidase with assay buffer) with 7.5 μM CaM dimer was added into the flow cells. Ca^{2+} or EGTA solution was changed by adding buffer to the flow cells. Fluorescent microtubule gliding was observed under epifluorescence by using an Olympus BX50 microscope equipped with a 3CCD camera (JK-TU53H; Toshiba, Japan).

3. Results and discussion

3.1. Design of kinesin mutants and CaM dimers using crosslinkers

In order to regulate movement of kinesin in a Ca^{2+}-dependent manner, we designed a kinesin monomer fused with CaM-binding peptide (K355–M13) and a CaM dimer (Fig. 1A). K355–M13 consists of the N-terminal motor domain, neck region, and M13 peptide; the latter containing a CaM target peptide at the C-terminus (Fig. 1B). We confirmed that ATPase activity of K355–M13 monomer was in a similar range as those of the wild-type kinesin (V_{max}, 38.42 ± 2.06 mol of Pi/s/moles of site; K_m[MT], 0.90 ± 0.17 μM [19]). We expected that CaM dimer binds individual M13 peptides of two K355–M13 fusion proteins in the presence of Ca^{2+}, thereby converting K355–M13 to the dimer configuration (Fig. 1A). Dimerization of K355–M13 via CaM homodimer formation should be reversed by removal of Ca^{2+}. Since kinesin-1 moves along microtubules as a dimer, we expected modulation of kinesin movement to be Ca^{2+}-dependent in our system. This hypothesis was tested in the experiments outlined below.

It has been demonstrated that the motility of kinesin is dependent on neck linker length [22]. Indeed, the movement of wild-type kinesin is decreased by changing the neck linker length. Therefore, we focused on the neck linker domain, which transmits intramolecular tension between the motor domains. The neck linker length of kinesin determines the distance between motor domains, and therefore alters motor activity. Since the CaM dimers are attached to the neck linker, it follows that variations in CaM conformation might also modulate motor activity of the associated K355–M13 construct. To test this, we designed three CaM constructs that have single cysteine mutations at the N-terminal (Q3C), center helix (R86C), or C-terminal (A147C) regions, respectively (Fig. 1C). We also prepared CaM dimers by forming a bridge between the mutant

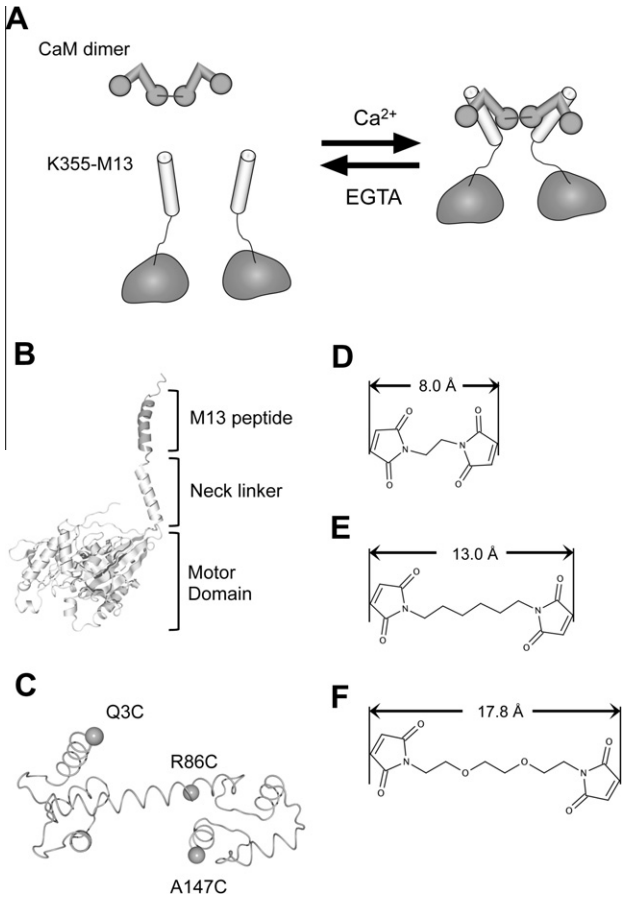

Fig. 1. Design of CaM dimer and K355–M13. (A) Schematic representation of Ca^{2+}-dependent reversible dimerization of kinesin using CaM dimer and K355–M13. (B) K355–M13 is composed of 407 amino acid (aa) residues: aa1–14, peptide linker; aa15–351, kinesin motor domain; aa352–368, kinesin neck linker; aa369–370, peptide linker; aa371–389, M13 peptide that binds to CaM; aa390–407, peptide linker and 6xHis tag. (C) Location of cysteine substitutions used for the crosslinking experiments. The α-carbon of the amino acids, Q3C (N-terminal region), R86C (center helix), and A147C (C-terminal region), respectively, substituted by cysteine are indicated in the space-filling model. The 3D structure was prepared using the molecular graphics program MolFeat with the coordinate date (PDB ID: 1CLL) of *Homo sapiens* calmodulin. (D–F) Dimaleimide crosslinker for covalent, irreversible conjugation between sulfhydryl groups. (D) BMOE, (E) BMH, and (F) $BM(PEO)_3$.

cysteine residues of two identical CaM mutants, using dimaleimide crosslinkers. Since the configuration of CaM is dumbbell-shaped, dimers produced as a result of crosslinking should exhibit significantly different configurations. The CaM mutant R86C dimer, where crosslinking occurs at the center helix region of CaM, should be X-shaped. On the other hand, CaM mutant Q3C or A147C dimers, where crosslinking occurs at N- or C-terminal region of CaM, respectively, should be M-shaped. We predicted that the difference in conformation of crosslinked CaM mutants, would therefore change the motility activities of the associated kinesin. As an additional test of whether CaM-dependent orientation of kinesin molecule motors changes their activity, we used three different lengths of crosslinker (BMOE (Fig. 1D) <BMH (Fig. 1E) <$BM(PEO)_3$ (Fig. 1F)). Together, this led to nine configurations of K355–M13 in complex with CaM dimers, which were tested for both on–off regulation of movement and changes in velocity.

3.2. Crosslinking of CaM mutants

In order to determine the optimal conditions for dimerization, we examined the relationship between crosslinker concentration and reaction time with the CaM mutants. The upper and bottom bands represent CaM dimer and CaM monomer, respectively. We found that dimerization of CaM R86C was highly efficient when the amount of BMOE was 0.5- or 0.75-fold that of the CaM mutant (Fig. 2A). This result indicates that the dimerization reaction was almost stoichiometric (CaM:crosslinker ≈ 2:1). We then conducted time course studies at a BMOE:CaM ratio of 2:1. Under these conditions, almost half of the total CaM was present in the dimeric form after 4 h (Fig. 2B). Similar results were observed with other crosslinkers (Fig. 2C–E) and with similar kinetics (Fig. 2F–H). These results indicate that CaM dimers were prepared effectively using crosslinkers.

3.3. Purification of CaM dimer

Since the dimerization reaction included a mix of CaM dimers and monomers, we further purified CaM dimers by SEC–HPLC. Fig. 3A shows the elution pattern before and after dimerization of the CaM mutant R86C with BMOE. Since these CaM mutants do not have tryptophan residues, we instead monitored the absorbance of peptide bonds at 230 nm. The elution time of the CaM monomer was 8.5 min, leading us to expect that CaM dimer would elute at an earlier time. Fig. 3B shows the SDS–PAGE analysis of the elution fractions (taken at 15-s intervals between 7 and 9.5 min) after the dimerization reaction was performed. The result of SDS–PAGE (Fig. 3B, lanes 3 and 4) indicates that the peak at 7.8 min is CaM dimer, and we therefore collected this fraction. The other CaM dimer variants were isolated in a similar manner.

3.4. Dimerization of K355–M13 induced by binding of CaM dimer

Next, we investigated whether CaM dimers induce K355–M13 dimerization. K355–M13 was reacted with BMOE-crosslinked CaM R86C in the presence of Ca^{2+} and dimerization was examined using SEC–HPLC (Fig. 3C). Since K355–M13 has tryptophan residues, we were able to monitor its elution from a mixture of K355–M13 monomers and CaM R86C–BMOE dimers, and found it to be 8.3 min. Since CaM-dimerized K355–M13 is larger than the K355–M13 monomer, we expected that demerit would elute earlier than 8.3 min. Fig. 3D shows the SDS–PAGE elution pattern (taken every 15 s from 6.25 min to 9.5 min) from the dimerization reaction of K355–M13 with CaM R86C–BMOE dimer. The result of the SDS–PAGE (Fig. 3D, lanes 3–6) indicates that the peak at 7.1 min is dimeric K355–M13 with CaM R86C–BMOE dimer, since these lanes include bands of CaM R86C–BMOE dimer, K355–M13 and the molar ratio of CaM R86C–BMOE dimer to K355–M13 is almost 1:2. We also confirmed that the peak at 7.1 min was not detected in the absence of Ca^{2+} (data not shown). These results demonstrate that the CaM dimer induces K355–M13 dimerization. We repeated these experiments using K355–M13 combined with other types of CaM dimers. We also confirmed that the ATPase activity of dimeric K355–M13 with CaM R86C–BMOE dimer (V_{max}, 43.12 ± 1.01 mol of Pi/s/mole of site; K_m[MT], 0.77 ± 0.25 μM) was approximately the same as those of the K355–M13 monomer or wild-type kinesin (V_{max}, 38.42 ± 2.06 mol of Pi/s/mole of site; K_m[MT], 0.90 ± 0.17 μM [19]). The ATPase activities of dimeric K355–M13 with the other CaM dimers were similar to those of the K355–M13 monomer or wild-type kinesin. This result demonstrates that K355–M13 ATPase activity is maintained upon dimerization and is not significantly altered in this Ca^{2+}-regulated system. The molecular weights of the CaM dimer and K355–M13 are 34 and 45 kDa, respectively. However, the elution time of the CaM dimer corresponded to an apparent molecular weight of 58 kDa, which is significantly higher than predicted. This phenomenon may be due to the steric structure induced by crosslinking of the dumbbell-shaped CaM monomers.

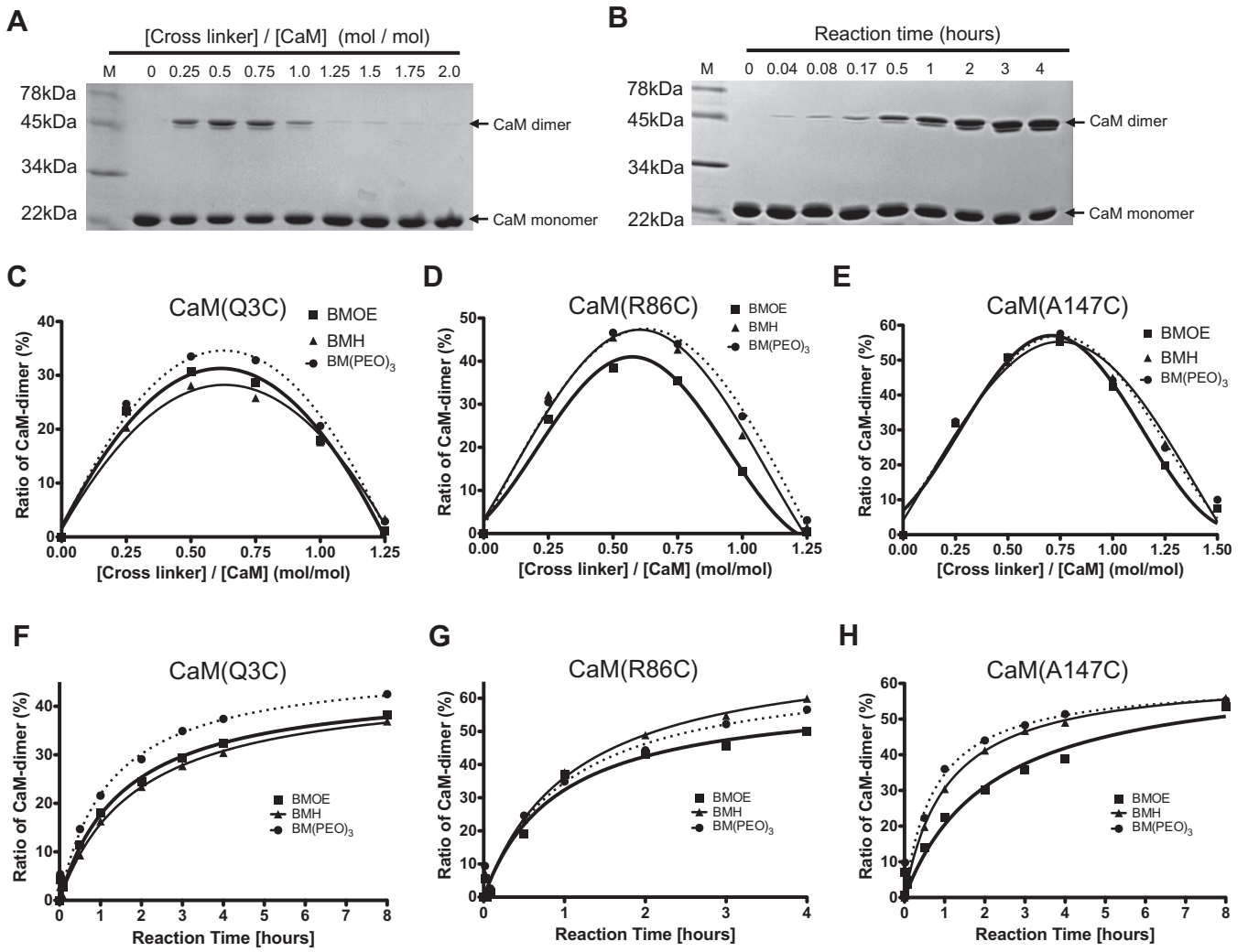

Fig. 2. CaM dimerization is dependent on crosslinker concentration and reaction duration SDS–PAGE of samples after dimerization of the CaM in the mixture containing (A) 50 μM CaM (R86C), 0–100 μM BMOE, 30 mM Tris–HCl (pH 7.5), and 30 mM NaCl at 25 °C for 4 h, or (B) 50 μM CaM (R86C), 25 μM BMOE, 30 mM Tris–HCl (pH 7.5), and 30 mM NaCl at 25 °C for 0–4 h. The samples were electrophoresed with SDS–PAGE after adding of 2 mM DTT for terminal dimerization. The arrows indicate CaM monomer and CaM dimer, respectively. The upper bands represent CaM dimers that migrate at approximately 45 kDa. The bottom bands represent CaM monomers that migrate at approximately 22 kDa. (C–E) Dimerization of CaM mutants Q3C (C), R86C (D) or A147C (E), is dependent on crosslinker concentration of crosslinkers, BMOE, BMH, or $BM(PEO)_3$, respectively. (F–H) Time course of CaM mutant Q3C (F), R86C (G), or A147C (H) dimerization with BMOE, BMH, or $BM(PEO)_3$ crosslinkers, respectively.

3.5. Ca^{2+}-dependent motility of engineered kinesin

Next, we examined whether K355–M13 in the presence of the CaM dimer displays reversible and Ca^{2+}-dependent molecular motor activity. We measured the velocities of microtubule gliding induced by K355–M13 with CaM dimers in the flow cell. Fig. 4A–C shows the velocity of K355–M13 with CaM dimers in the presence or absence of Ca^{2+}. As expected, K355–M13 with CaM dimer was motile in the presence of Ca^{2+}, and static in its absence. The alterations in velocity induced by changing Ca^{2+} concentration were reversible, and retained even over multiple Ca^{2+} changes. This was true for all CaM dimers (Fig. 4A–C). As controls, we also measured the velocities for K355–M13 alone or K355–M13 with CaM wild type (monomer). No motility was observed either in the presence or absence of Ca^{2+} (data not shown), which is consistent with their inability to spontaneously form dimers. These results clearly demonstrated that the K355–M13 can act as reversible, Ca^{2+}-dependent reversible molecular motor when induced to dimerize by CaM.

Interestingly, the velocity of microtubule gliding was dependent on the crosslinkage positions of the CaM mutants (Fig. 4A–C). K355–M13 with CaM R86C–BMOE dimer and CaM A147C–BMOE dimer exhibited the highest and the lowest motility activity, respectively. The neck linker domains transmit the inter-head mechanical forces that underlie coordination of their hydrolysis cycles into both motor domains [23]. It is plausible that their internal forces are transmitted through M13 peptide, CaM dimer, and neck linker in the case of K355–M13 with CaM dimer. Therefore, we propose that transmission of internal forces is affected by presence of the M13 peptide, as well as the composition and conformation of the CaM dimer. This hypothesis is supported by our observation that K355–M13 in the presence of the CaM dimer moves slower than wild-type K560 (550 ± 140 nm [24]). The velocity of kinesin is proportionate to the transmission strength of the internal forces between the two heads of kinesin [25]. Therefore, we suggest that the M13 peptide and CaM dimer are less efficient in transmission between the kinesin heads when compared with the α-helical coiled-coil stalk found in unmodified kinesin. By the same reasoning, we infer from our data that K355–M13 with the CaM R86C–BMOE dimer transmits internal forces more efficiently than K355–M13 with the CaM A147C–BMOE dimer. In addition to the effect of CaM conformation, the velocities

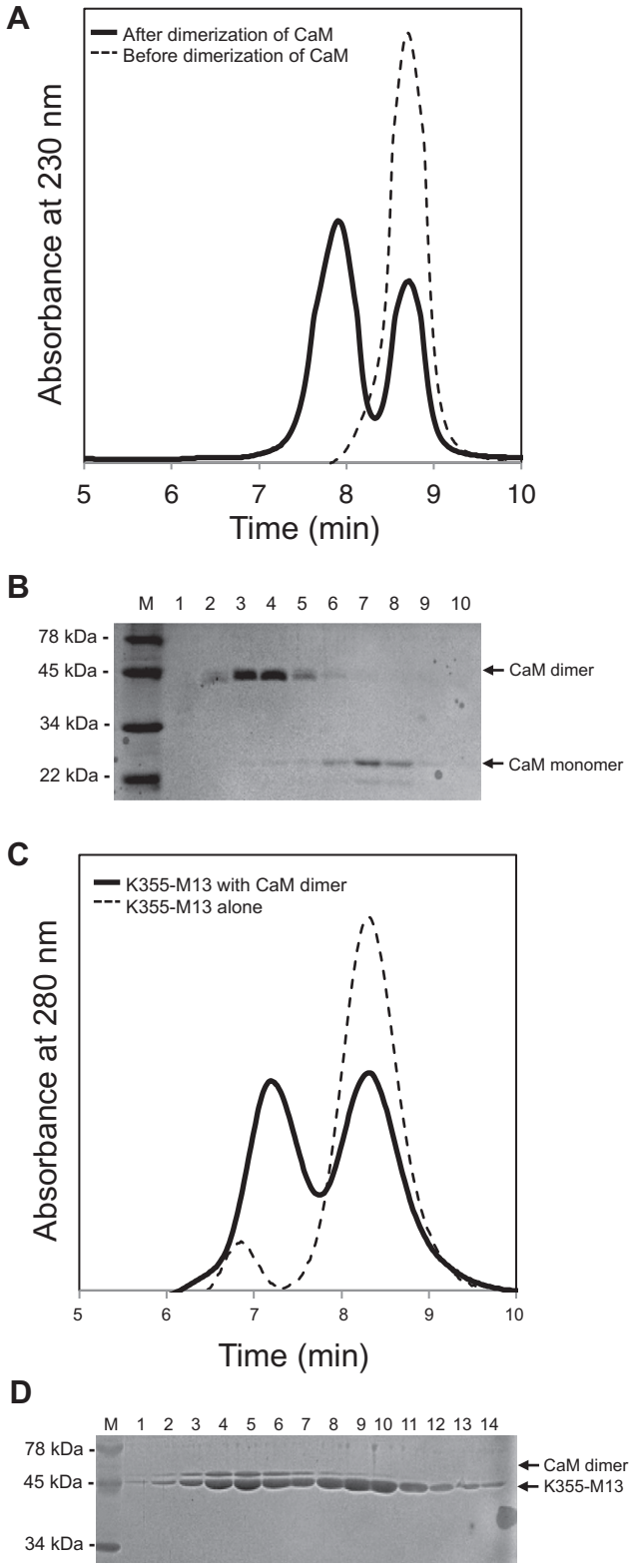

Fig. 3. Isolation of CaM dimers or K355–M13 with CaM dimer by SEC–HPLC. Isolation of the CaM R86C mutant alone or following BMOE-mediated dimerization (A, broken and solid lines, respectively) or (C) K355–M13 alone or following BMOE-mediated dimerization (broken and solid lines, respectively). Absorbance was measured at 230 nm (A) or 280 nm (C) in the presence of Ca^{2+}. Eluted fractions of the dimerization reaction solution of CaM mutant (R86C) with BMOE (B), or dimerization reaction solution of K355–M13 with CaM R86C–BMOE (D) was analyzed by SDS–PAGE. M, molecular weight markers; other lanes are eluted taken every 15 s from (B) between 7 and 9.5 min or (D) 6.25 and 9.75 min. The arrows indicate (B) CaM monomers and CaM dimers, and (D) K355–M13 and CaM dimers, respectively.

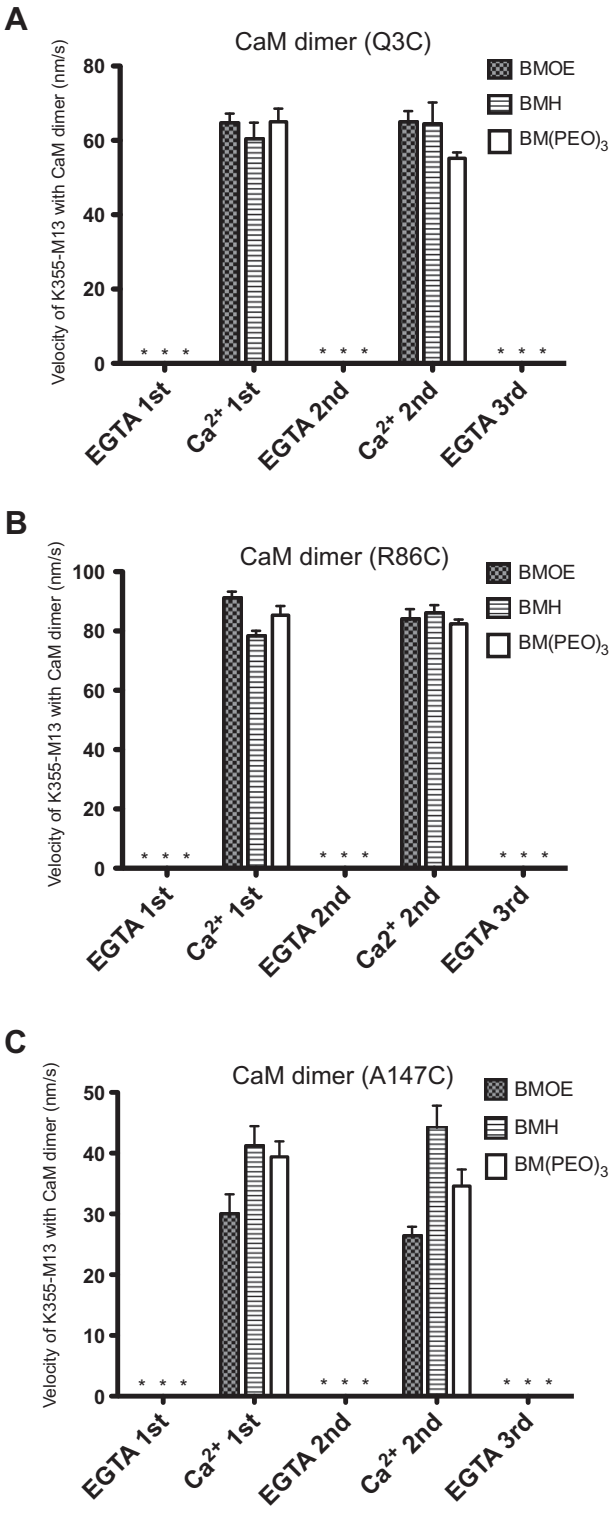

Fig. 4. Reversible Ca^{2+}-dependent motor activity of K355–M13 with CaM dimer. CaM mutant dimers Q3C (A), R86C (B), or A147C (C) with BMOE, BMH, or $BM(PEO)_3$, were added into flow cells coated with K355–M13 with rhodamine-labeled microtubules in the presence of Ca^{2+} or EGTA. Asterisks indicate that the velocity of K355–M13 with the CaM mutant dimer is 0 nm/s. Error bars indicate SE of velocities of >10 microtubules in the microtubule gliding assay.

change as crosslinker lengths varied, particularly with the CaM A147C mutant dimer (Fig. 4C).

The Ca^{2+}/CaM system is very stable and exhibits excellent on–off properties, making it suitable for other functional biomolecular

systems. Another possible approach may be the use of photo-controlled CaM. We previously synthesized a photochromic crosslinker, 4,4′-azobenzene-dimaleimide (ABDM), that undergoes reversible *cis–trans* isomerization upon UV and VIS light irradiation resulting in a change in crosslinking length from 5 to 17 Å [26]. Furthermore, we have also achieved photocontrolled interaction of CaM with M13 peptide using photochromic compounds [18]. Therefore, both UV and VIS light irradiation could be used to modulate the velocity of K355–M13 with CaM–ABDM mutant dimer. This approach holds great promise as an accelerator and brake system for molecular shuttles used in the bionanotechnology field.

Acknowledgment

This work was supported by Grant-in-Aid for Research Activity Start-up (22870030).

References

[1] H. Hess, V. Vogel, Molecular shuttles based on motor proteins: active transport in synthetic environments, J. Biotechnol. 82 (2001) 67–85.
[2] H. Hess, G.D. Bachand, V. Vogel, Powering nanodevices with biomolecular motors, Chemistry 10 (2004) 2110–2116.
[3] M.G. van den Heuvel, C. Dekker, Motor proteins at work for nanotechnology, Science 317 (2007) 333–336.
[4] H. Hess, Engineering applications of biomolecular motors, Annu. Rev. Biomed. Eng. 13 (2011) 429–450.
[5] A. Agarwal, H. Hess, Biomolecular motors at the intersection of nanotechnology and polymer science, Prog. Polym. Sci. 35 (2010) 252–277.
[6] T. Fischer, A. Agarwal, H. Hess, A smart dust biosensor powered by kinesin motors, Nat. Nanotechnol. 4 (2009) 162–166.
[7] G. Muthukrishnan, B.M. Hutchins, M.E. Williams, W.O. Hancock, Transport of semiconductor nanocrystals by kinesin molecular motors, Small 2 (2006) 626–630.
[8] H. Shishido, K. Nakazato, E. Katayama, S. Chaen, S. Maruta, Kinesin–calmodulin fusion protein as a molecular shuttle, J. Biochem. 147 (2010) 213–223.
[9] H. Higuchi, E. Muto, Y. Inoue, T. Yanagida, Kinetics of force generation by single kinesin molecules activated by laser photolysis of caged ATP, Proc. Natl. Acad. Sci. USA 94 (1997) 4395–4400.
[10] K. Konishi, T.Q. Uyeda, T. Kubo, Genetic engineering of a Ca(2+) dependent chemical switch into the linear biomotor kinesin, FEBS Lett. 580 (2006) 3589–3594.
[11] J. Howard, A.J. Hudspeth, R.D. Vale, Movement of microtubules by single kinesin molecules, Nature 342 (1989) 154–158.
[12] S.M. Block, L.S. Goldstein, B.J. Schnapp, Bead movement by single kinesin molecules studied with optical tweezers, Nature 348 (1990) 348–352.
[13] E. Meyhofer, J. Howard, The force generated by a single kinesin molecule against an elastic load, Proc. Natl. Acad. Sci. USA 92 (1995) 574–578.
[14] S. Adio, J. Reth, F. Bathe, G. Woehlke, Review: regulation mechanisms of kinesin-1, J. Muscle Res. Cell Motil. 27 (2006) 153–160.
[15] D. Chin, A.R. Means, Calmodulin: a prototypical calcium sensor, Trends Cell Biol. 10 (2000) 322–328.
[16] A. Persechini, P.M. Stemmer, Calmodulin is a limiting factor in the cell, Trends Cardiovasc. Med. 12 (2002) 32–37.
[17] D.K. Blumenthal, K. Takio, A.M. Edelman, H. Charbonneau, K. Titani, K.A. Walsh, E.G. Krebs, Identification of the calmodulin-binding domain of skeletal muscle myosin light chain kinase, Proc. Natl. Acad. Sci. USA 82 (1985) 3187–3191.
[18] H. Shishido, M.D. Yamada, K. Kondo, S. Maruta, Photocontrol of calmodulin interaction with target peptides using azobenzene derivative, J. Biochem. 146 (2009) 581–590.
[19] M.D. Yamada, Y. Nakajima, H. Maeda, S. Maruta, Photocontrol of kinesin ATPase activity using an azobenzene derivative, J. Biochem. 142 (2007) 691–698.
[20] D.D. Hackney, Kinesin ATPase: rate-limiting ADP release, Proc. Natl. Acad. Sci. USA 85 (1988) 6314–6318.
[21] G. Woehlke, A.K. Ruby, C.L. Hart, B. Ly, N. Hom-Booher, R.D. Vale, Microtubule interaction site of the kinesin motor, Cell 90 (1997) 207–216.
[22] S. Shastry, W.O. Hancock, Neck linker length determines the degree of processivity in kinesin-1 and kinesin-2 motors, Curr. Biol. 20 (2010) 939–943.
[23] S. Shastry, W.O. Hancock, Interhead tension determines processivity across diverse N-terminal kinesins, Proc. Natl. Acad. Sci. USA 108 (2011) 16253–16258.
[24] R.B. Case, D.W. Pierce, N. Hom-Booher, C.L. Hart, R.D. Vale, The directional preference of kinesin motors is specified by an element outside of the motor catalytic domain, Cell 90 (1997) 959–966.
[25] Y. Miyazono, M. Hayashi, P. Karagiannis, Y. Harada, H. Tadakuma, Strain through the neck linker ensures processive runs: a DNA–kinesin hybrid nanomachine study, EMBO J. 29 (2010) 93–106.
[26] N. Umeki, T. Yoshizawa, Y. Sugimoto, T. Mitsui, K. Wakabayashi, S. Maruta, Incorporation of an azobenzene derivative into the energy transducing site of skeletal muscle myosin results in photo-induced conformational changes, J. Biochem. 136 (2004) 839–846.